Synthesis and Microwave Dielectric Properties of $(Ce_{1-y}Dy_y)(Nb_{1-x}Ta_x)TiO_6$ Ceramics

Takeshi Oishi[1], Hirotaka Ogawa[1], Akinori Kan[1] and Hitoshi Ohsato[2]

[1]Faculty of Science and Technology, Meijo University, 1-501 Shiogamaguchi, Tempaku-ku, Nagoya 468-8502, Japan
[2]Materials Science and Engineering, Shikumi College, Nagoya Institute of Technology, Gokiso-cho, Showa-ku, Nagoya 466-8555, Japan

Abstract

The effects of the Ta substitution for Nb and the Dy substitution for Ce on the microwave dielectric properties and crystal structure of $(Ce_{1-y}Dy_y)(Nb_{1-x}Ta_x)TiO_6$ ceramics were investigated in this study. In the case of the Ta substitution for Nb in the $CeNbTiO_6$ ceramic, a single phase of aeschynite-type structure was obtained over the whole composition range. On the other hand, the XRPD patterns of $(Ce_{1-y}Dy_y)(Nb_{0.5}Ta_{0.5})TiO_6$ ceramics with the composition y ranging from 0 to 0.625 show a single phase which corresponds to the aeschynite-type structure, whereas those of the samples at the composition higher than y=0.85 exhibit the euxenite-type structure. In the composition range of 0.65-0.85, the phase transition took place; the aeschynite and euxenite phases coexisted. The dielectric constant of $(Ce_{1-y}Dy_y)(Nb_{0.5}Ta_{0.5})TiO_6$ ceramics decreased from 44.5 to 15.9, while the quality factor increased from 13398 to 31753GHz with the Dy substitution for Ce. The temperature coefficient of resonant frequency of the ceramics varied from 79.8 to –42.9ppm/□; a near zero temperature coefficient of resonant frequency results in the composition of y=0.75 with a dielectric constant of 30.9 and Q□f value of 23708GHz. These variations in the microwave dielectric properties of $(Ce_{1-y}Dy_y)(Nb_{0.5}Ta_{0.5})TiO_6$ ceramics are attributed to the phase transition of ceramics from aeschynite-type structure to euxenite-type structure.

Keywords: Powders-solid state reaction method, X-ray method, Dielectric properties, Electron microscopy

Introduction

The microwave dielectric ceramics for the application as a resonator must have a high dielectric constant (ε_r), a high quality factor (Q□f) and a near zero temperature coefficient of resonant frequency (τ_f). Recently, the microwave dielectric properties of $CeNbTiO_6$ ceramic which has an aeschynite-type structure [1] were reported to have a ε_r of 54, a Q□f value of 6530GHz and τ_f value of 67ppm/□[2]; the dielectric constant of the ceramic is comparable to that of $Ba_2Ti_9O_{20}$ ceramic [3] which is widely used for the dielectric resonator in the base station. However, since the Q□f value of $CeNbTiO_6$ ceramic is lower than

that of $Ba_2Ti_9O_{20}$ ceramic, an improvement in the $Q \times f$ value of $CeNbTiO_6$ ceramic is required for a commercial application. Moreover, the τ_f value of $CeNbTiO_6$ ceramic has been reported to possess a large positive value [2]; the improvement in τ_f value is also required. Thus, in order to improve these dielectric properties, the influence of Ta substitution for Nb and Dy substitution for Ce on the microwave dielectric properties and crystal structure of $CeNbTiO_6$ ceramic has been investigated in this study. Moreover, the relationship between the structural phase transition and microwave dielectric properties of $(Ce_{1-y}Dy_y)(Nb_{0.5}Ta_{0.5})TiO_6$ ceramics was also investigated by using the Rietveld analysis [4,5] because it was known that the crystal structure of $CeNbTiO_6$ ceramic had the aeschynite-type structure, whereas the $DyNbTiO_6$ ceramic had the euxenite-type structure[1]; the details on these relationships have not been clarified to date.

Experimental

High purity (≥99.9%) CeO_2, Dy_2O_3, Nb_2O_5, Ta_2O_5 and TiO_2 powders weighed on the basis of the stoichiometric composition, i.e., $(Ce_{1-y}Dy_y)(Nb_{1-x}Ta_x)TiO_6$, were mixed with acetone and calcined at 1250□ for 6h in air by the conventional solid-state reaction method. These calcined powders were crushed and ground with polyvinyl alcohol, and then formed into pellets of 12mm in diameter and 7mm thick under a pressure of 100MPa. These pellets were sintered at the various temperatures ranging from 1350°to 1500□ for 10h in air with heating and cooling rates of 5□/min. Subsequently, these pellets were polished and annealed at 850□ for 2h in air. The phases of the sintered specimens were identified by using the X-ray powder diffraction (XRPD); the crystal structures of the ceramics were refined in terms of the Rietveld analysis. Phase composition analysis and morphology microanalysis of the sintered samples were investigated by using a field emission scanning electron microscopy (FE-SEM) and energy-dispersive X-ray (EDX) spectroscopy. The microwave dielectric properties (ε_r and $Q \times f$) in the frequency range of 5.4-10.1GHz were examined by the Hakki and Coleman method [6]. The temperature coefficient of resonant frequency of the sample was determined from the resonant frequency at the two temperatures of 20°and 80□.

Results and discussion

Figure 1 shows the XRPD patterns of $Ce(Nb_{1-x}Ta_x)TiO_6$ ceramics sintered in the temperature range of

1350°-1500□; no secondary phase was detected over the whole composition range. In order to clarify the effect of Ta substitution for Nb on the crystal structure of $Ce(Nb_{1-x}Ta_x)TiO_6$ ceramics, the lattice parameters of the samples were refined by the Rietveld analysis and the results are shown in Fig.2 as a function of composition *x*. A linear dependence of lattice parameter on the composition *x* was observed; the lattice parameter, *a*, linearly decreased with the Ta substitution for Nb, whereas the lattice parameter, *c*, increased. However, the remarkable variations in the lattice parameter, *b*, were not observed with the Ta substitution for Nb. From the results of variations in the lattice parameters, it is considered that the $Ce(Nb_{1-x}Ta_x)TiO_6$ ceramics form the solid solutions because the linear variations in the lattice parameters satisfy the Vegard's low which confirms the formation of solid solutions.

The influences of Ta substitution for Nb on the microwave dielectric properties of $Ce(Nb_{1-x}Ta_x)TiO_6$ solid solutions are listed in Table□. The dielectric constants of the solid solutions decreased from 52.7 to 35.6, whereas the $Q\square f$ values slightly increased from 10702 to 14616GHz by the Ta substitution for Nb. Moreover, the temperature coefficients of resonant frequency of the solid solutions ranged from 91.8 to 72.0ppm/□. Although the Ta substitution for Nb leads to the slight increase in $Q\square f$ value of the solid solutions, a high $Q\square f$ value with a τ_f value that closes to 0ppm/□ is required for a commercial application. In order to improve these dielectric properties of the solid solutions, Dy substitution for Ce was performed for the $Ce(Nb_{0.5}Ta_{0.5})TiO_6$ compound because the sintering temperature of $Ce(Nb_{1-x}Ta_x)TiO_6$ solid solutions was increased from 1350°to 1500□; it may be difficult to obtain the well-sintered specimens at the Ta rich region, though the Ta rich phase has a high $Q\square f$ value in comparison with that of the Nb rich phase.

Figure 3 shows the XRPD patterns of $(Ce_{1-y}Dy_y)(Nb_{0.5}Ta_{0.5})TiO_6$ ceramics. The XRPD patterns of the samples in the composition range of 0-0.625 showed a single phase which corresponded to the aeschynite-type structure (S.G. *Pnma*). On the other hand, at the composition higher than y=0.85, the single phase of euxenite-type structure (S.G. *Pbcn*) was obtained. Moreover, two phases, i.e., aeschynite and euxenite phases, coexisted in the composition ranging from 0.65 to 0.85; the structural phase transition was observed with the Dy substitution for Ce.

The relationship between the Dy substitution for Ce and the phase transition in the composition range of 0.65-0.85 was also investigated in terms of the Rietveld analysis; thus, the weight fraction of the each phase which was detected in the XRPD patterns was determined by using the following equation:

$$W_p = S_p(ZMV)_p \Big/ \sum_i S_i(ZMV)_i \quad (1)$$

where *S*, *Z*, *M* and *V* are the scale factor of the Rietveld analysis, the number of formula unit per unit cell, the mass of the formula and the unit cell volume, respectively. This method is widely used to estimate the weight fraction of the phases [7]; the weight fractions of aeschynite and euxenite phases were shown Fig.4 as a function of the composition *y*. The weight fraction of aeschynite phase decreased, whereas that of euxenite phase increased with increasing composition *y* from 0.65 to 0.85.

As for the relationship between the structural phase transition and microstructure, the FE-SEM observations of the samples at *y*=0, 0.75 and 1 were performed; the micrographs of these samples were shown in Fig.5. At *y*=0, i.e., the aeschynite phase region, the image shows a rectangle-like grain structure, whereas the microstructure of sample at *y*=1 (euxenite-type structure) has a typical equiaxed grain structure. On the other hand, at *y*=0.75, the two-type grain structures, i.e., the aeschynite-type and euxenite-type grain structures, were observed in the micrograph; this result agrees with the that of XRPD. Thus, it is found that the phase transition from aeschynite phase to euxenite phase takes place the morphological changes in the samples.

In the single phase region, i.e., $0 \le y \le 0.625$ and $0.875 \le y \le 1$, the crystal structure analysis of the samples was carried out in order to clarify the relationship between the differences in the crystal structure and microwave dielectric properties. The refined lattice parameters and unit cell volumes of aeshynite structure ($0 \le y \le 0.625$) and euxenite structure ($0.875 \le y \le 1$) were listed in Table□. The lattice parameters, *b* and *c*, of aeschynite structure decreased with increased composition *y*, whereas the lattice parameter, *a*, increased. As a result, the unit cell volumes of the samples decreased; these results were related to the differences in the ionic radii between Ce^{3+} and Dy^{3+} ions because the ionic radius of Dy^{3+} ion is smaller than that of Ce^{3+} ion when the coordination number is eight [8]. Moreover, in the case of euxenite-type structure, all the lattice parameter of the samples decreased with increased composition *y* up to *y*=1. The crystal structure of aeschynite phase is composed of the CeO_8 polyhedron and the $(Nb,Ta,Ti)O_6$ octahedron, whereas that of euxenite phase contains the $(Ce,Dy)O_8$ polyhedron and the $(Nb,Ta,Ti)O_6$ octahedron; these polyhedra are shown in Fig.6. The effects of Dy substitution for Ce on the volume of polyhedra in the $(Ce_{1-y}Dy_y)(Nb_{0.5}Ta_{0.5})TiO_6$ ceramics are shown in Fig.7 as a function of composition *y*. Although any remarkable variations in the volume of the $(Nb,Ta,Ti)O_6$ octahedra were not observed for the composition *y*, a linear

dependence of volume in the $(Ce,Dy)O_8$ polyhedra on composition y was observed; the volume of the $(Ce,Dy)O_8$ polyhedra decreased with increasing composition y. Thus, the decrease in the unit cell volume of the $(Ce_{1-y}Dy_y)(Nb_{0.5}Ta_{0.5})TiO_6$ in the single phase region is considered to relate with the variations in the volume of $(Ce,Dy)O_8$ polyhedra.

Although the relationship between the Dy substitution for Ce and the volume of polyhedra was clarified, the effect of Dy substitution for Ce on the variations in the covalency of cation-oxygen bonds has not been investigated; it is considered that these variations in the covalancy exert an influence on the structural phase transition and microwave dielectric properties. Thus, the varations in the covalency of cation-oxygen bond in single phase region ($0 \le y \le 0.625$, $0.875 \le y \le 1$) was calculated by using the refined bond length and the relationship between covalency and bond length is given by two equations:

$$s = (R/R_1)^{-N} \quad (2)$$

$$f_c' = as^M \quad (3)$$

where s, R, R_1 and N are bond strength, refined bond length, empirical constant which depends on the cation site, and the constant which is different for each cation-anion pair, respectively; in this case, N=6.0. In addition, f'_c, a and M in eq.(3) indicate the covalence of the cation-oxygen bond and empirical constants which depend on the number of electron. The values of these parameters and the detail on the relationship between the covalency and bond strength are given elsewhere [9]; the covalency of cation-oxygen bond in the $(Ce,Dy)O_8$ polyhedra obtained in this study is shown in Fig.8 as a function of composition y. In the region□, i.e., aeschynite structure, the covalencies of all the (Ce,Dy)-O bonds increased with the Dy substitution for Ce; in the euxenite structure (region□ in Fig.8), the covalency of (Ce,Dy)-O bonds also increased, though only the covalency of (Ce,Dy)-O2 bond decreased. The increase in the covalency of (Ce,Dy)-O bonds in the $(Ce,Dy)O_8$ polyhedron is due to the decrease in the bond length of (Ce,Dy)-O which arises from the difference in the ionic radii between the Ce^{3+} and Dy^{3+} ions; the decrease in the volume of $(Ce,Dy)O_8$ polyhedra as mentioned above implies the decrease in the (Ce,Dy)-O bond length. As for the variations in the covalncy of (Nb,Ta,Ti)-O bonds in the octahedra, any significant variations in the covalency were not recognized in aeschynite and euxenite structures; thus, this suggests that the Dy substitution for Ce primarily exerts an influence on the covalency of (Ce,Dy)-O bond in $(Ce,Dy)O_8$ polyhedron.

The microwave dielectric properties, i.e., ε_r, $Q\square f$ and τ_f, of $(Ce_{1-y}Dy_y)(Nb_{0.5}Ta_{0.5})TiO_6$ ceramics are shown in Figs.9 and 10 as a function of composition y. Comparing the microwave dielectric properties of aeschynite-type phase at y=0 with those of euxenite-type phase at y=1, some remarkable differences in the microwave dielectric properties due to the structural phase transition were observed; the aeschynite-type phase has a high dielectric constant and a low $Q\square f$ values with a positiveτ_f value in comparison with the ε_r and $Q\square f$ values of euxenite-type phase. With increasing composition y, the dielectric constant of the samples in regions□ and □ decreased, whereas the $Q\square f$ values of the samples increased; as a result, a maximum $Q\square f$ value of 31753GHz was obtained in the euxenite-type phase at y=1. The linear dependence of ε_r and $Q\square f$ values on the composition y in regions□ and □ may relate with the variations in the covalency of (Ce,Dy)-O bonds in the $(Ce,Dy)O_8$ polyhedra because these dielectric properties and covalency showed a similar tendency for the composition y. At $0.65 \leq y \leq 0.85$, the dielectric constant of the samples decreased from 40.4 to 20.0, whereas the $Q\square f$ value slightly increased. Moreover, theτ_f value of the samples ranged from 41.1 to –40.3ppm/□; a near zero temperature coefficient of resonant frequency was achieved at approximatly y=0.75 with a dielectric constant of 30.9 and a $Q\square f$ value of 23708GHz. Thus, it was found that a temperature-stable ceramics can be obtained by coexisting the aeschynite and euxenite phases; these variations in the microwave dielectric properties in the composition range of 0.65 to 0.85 are considered to be strongly influenced by the weight fraction of aeschynite and euxenite phases.

Conclusion

The $(Ce_{1-y}Dy_y)(Nb_{1-x}Ta_x)TiO_6$ ceramics were prepared and the relationships between the crystal structure and microwave dielectric properties were investigated. From crystal structure analysis, it was found that the Ta substitution for Nb in $Ce(Nb_{1-x}Ta_x)TiO_6$ ceramics showed a single phase of aeschynite-type structure over the whole composition range. On the other hand, the phase transition from aeschynite-type to euxenite-type phases was observed when the Dy substitution for Ce was performed in $(Ce_{1-y}Dy_y)(Nb_{0.5}Ta_{0.5})TiO_6$ ceramics; the single phase of aeschynite-type structure was observed in the composition range of 0-0.625, whereas the that of euxenite-type structure appeared at the compositions higher than y=0.85. The evaluation of covaleny of the cation-oxygen bond in these single phase regions revealed that the Dy substitution for Ce enhanced the increase in covalency of cation-oxygen bonds in $(Ce,Dy)O_8$ polyhedra because the decrease in the (Ce,Dy)-O bonds resulted from the difference in the ionic

radii between Ce^{3+} and Dy^{3+} ions. The microwave dielectric properties of $(Ce_{1-y}Dy_y)(Nb_{0.5}Ta_{0.5})TiO_6$ ceramics strongly depended on the difference in the crystal structure between aeschynite and euxenite-type structures; in the composition range of 0.65-0.85, the weight fraction of aeschynite and euxenite phases exerts an influence on the variations in the microwave dielectric properties. As a result, a near zero τ_f value of $(Ce_{1-y}Dy_y)(Nb_{0.5}Ta_{0.5})TiO_6$ ceramics was obtained at approximately y=0.75.

References

1. Chang, P. -S., Dimorphs and Isomorphs in $CeNbTiO_6$-$YNbTiO_6$. *Sci. Sin.,* 1963, **12**, 2337-2343.
2. Sebastian, M. T. Solomon, S. Ratheesh, R. George, J. and Mohanan, P., Preparation, Characterization and Microwave Properties of $RETiNbO_6$ (RE = Ce, Pr, Nd, Sm, Eu, Gd, Tb, Dy, Y and Yb) Dielectric Ceramics. *J. Am. Ceram. Soc*., 2001, **84,** 1487-1489.
3. O'Bryan, H. M., Jr. and Thomson, J., Jr. Phase Equilibriums in the Titanium Oxide-Rich Region of the System Barium Oxide-titanium Oxide. *J. Am. Ceram. Soc*., 1974, **57,** 522-526.
4. Rietveld, H. M., Profile Refinement Method for Nuclear and Metal Urinates. *J. Appl. Crystallogr*., 1969, **2,** 65-71.
5. Izumi, F., Rietveld Method, ed. R. A. Young. Oxford University Press, Oxford, 1993. Chapter 13.
6. Hakki, B. W. and Coleman, P. D., A Dielectric Resonator Method of Measuring Inducrive in the Millimeter Range. *IRE Trans. Microwave Theory & Tech*., 1960, **MTT-8,** 402-410.
7. Hill, R. J. and Howard, C. J., Quantitative Phase Analysis from Neutron Powder Diffraction Data using the Rietveld Method. *J. Appl. Cryst*., 1978, **20,** 467-474.
8. Shannon, R. D., Revised Effective Ionic Radii and Systematic Studies of Interatomic Distance in Halides and Chalcogemides. *Acta. Cryst*., 1976, **A32,** 751-767.
9. Brown, I. D. and Shannon, R. D., Empirical Bond-strength Bond-length Curves for Oxides. *Acta. Cryst*., 1973, **A29,** 266-282.

Figure Captions

Fig.1 XRPD patterns of $Ce(Nb_{1-x}Ta_x)TiO_6$ solid solutions at (a) x=0, (b)x=0.5 and (c) x=1.

Fig.2 Effect of Ta substitution for Nb on lattice parameters of $Ce(Nb_{1-x}Ta_x)TiO_6$ solid solutions as a function of composition x.

Fig.3 XRPD patterns of $(Ce_{1-y}Dy_y)(Nb_{0.5}Ta_{0.5})TiO_6$ ceramics at (a) y=0, (b) y=0.625, (c) y=0.75, (d) y=0.875 and (e) y=1.

Fig.4 Weight fractions of aeschynite and euxenite structures.

Fig.5 FE-SEM photographs of $(Ce_{1-y}Dy_y)(Nb_{0.5}Ta_{0.5})TiO_6$ ceramics at (a) y=0, (b) y=0.75 and (c) y=1.

Fig.6 The crystal structure of (a) CeO_8 polyhedron, (b) $(Ce,Dy)O_8$ polyhedron and (c) $(Nb,Ta,Ti)O_6$ octahedron.

Fig.7 Variations in volume of $(Ce,Dy)O_8$ polyhedron and $(Nb,Ta,Ti)O_6$ octahedron.

Fig.8 Effect of Dy substitution for Ce on covalency of R-O (R=Ce,Dy) bonds as a function of composition y.

Fig.9 Variations in dielectric constant and $Q \times f$ values of $(Ce_{1-y}Dy_y)(Nb_{0.5}Ta_{0.5})TiO_6$ ceramics as a function of composition y.

Fig.10 Temperature coefficient of resonant frequency of $(Ce_{1-y}Dy_y)(Nb_{0.5}Ta_{0.5})TiO_6$ ceramics.

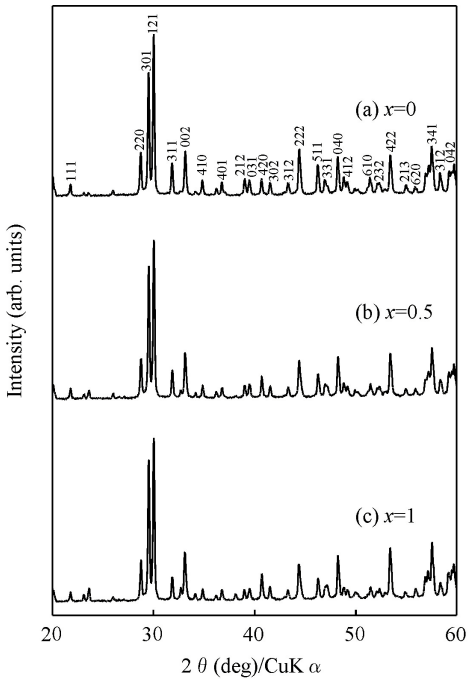
Intensity (arb. units)
(a) x=0
(b) x=0.5
(c) x=1
111
220
301
121
311
002
410
401
212
031
420
302
312
222
511
331
040
412
610
252
422
213
620
341
312
042
20
30
40
50
60
2 θ (deg)/CuK α

Fig.1

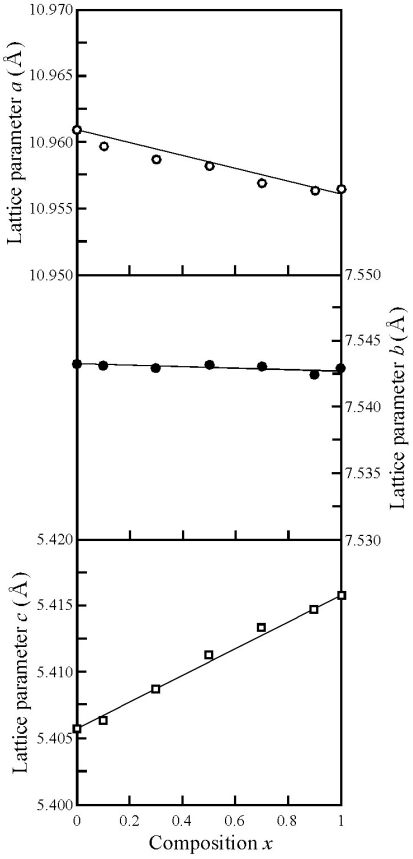
10.970
10.965
10.960
10.955
10.950
Lattice parameter a (Å)
7.550
7.545
7.540
7.535
7.530
Lattice parameter b (Å)
5.420
5.415
5.410
5.405
5.400
Lattice parameter c (Å)
0
0.2
0.4
0.6
0.8
1
Composition x

Fig.2

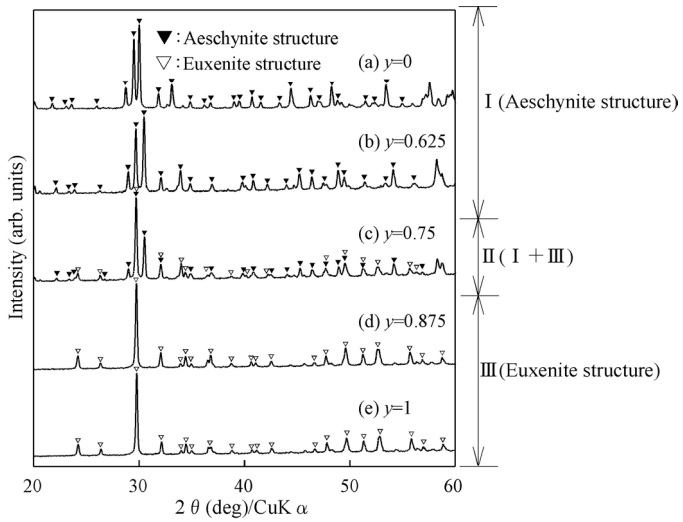
▼: Aeschynite structure
▽: Euxenite structure
(a) y=0
(b) y=0.625
(c) y=0.75
(d) y=0.875
(e) y=1
I (Aeschynite structure)
II (I + III)
III (Euxenite structure)
Intensity (arb. units)
20
30
40
50
60
2 θ (deg)/CuK α

Fig.3

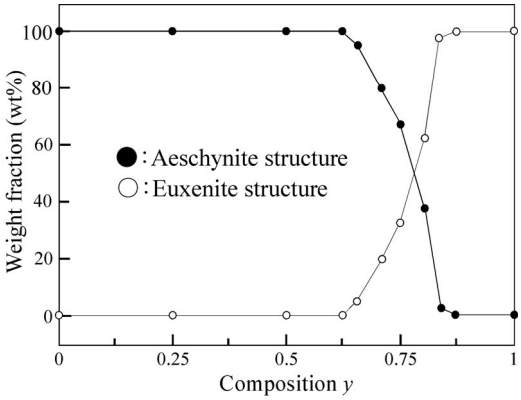
100
80
60
40
20
0
Weight fraction (wt%)
●: Aeschynite structure
○: Euxenite structure
0
0.25
0.5
0.75
1
Composition y

Fig.4

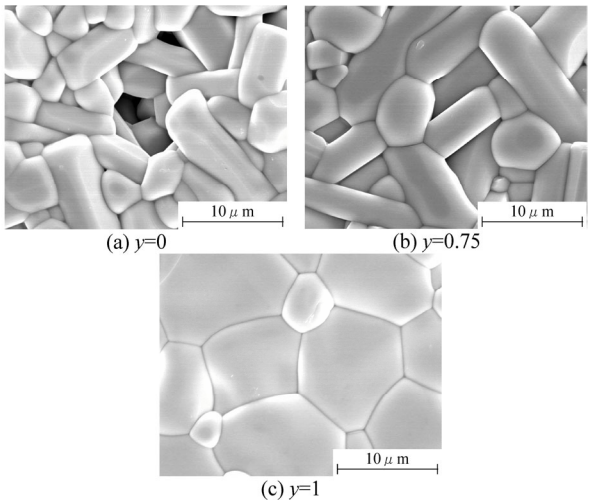

(a) y=0 (b) y=0.75

(c) y=1

Fig.5

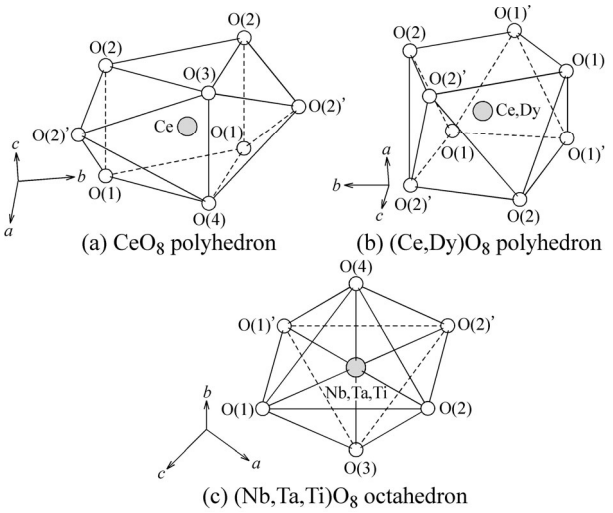
O(2)
O(2)
O(3)
O(2)'
Ce
O(2)'
O(1)
c
b
O(1)
a
O(4)
(a) CeO8 polyhedron
O(1)'
O(2)
O(1)
O(2)'
Ce,Dy
O(1)
O(1)'
a
b
c
O(2)'
O(2)
(b) (Ce,Dy)O8 polyhedron
O(4)
O(1)'
O(2)'
b
Nb,Ta,Ti
O(1)
O(2)
c
a
O(3)
(c) (Nb,Ta,Ti)O8 octahedron

Fig.6

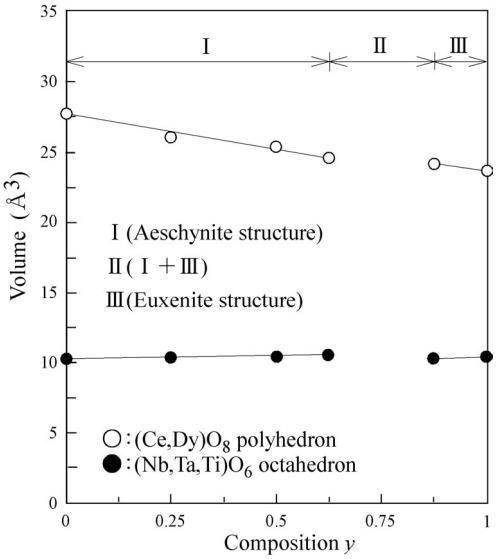
I
II
III
Volume (Å3)
Composition y
I (Aeschynite structure)
II (I + III)
III (Euxenite structure)
○ : (Ce,Dy)O8 polyhedron
● : (Nb,Ta,Ti)O6 octahedron
0
5
10
15
20
25
30
35
0
0.25
0.5
0.75
1

Fig.7

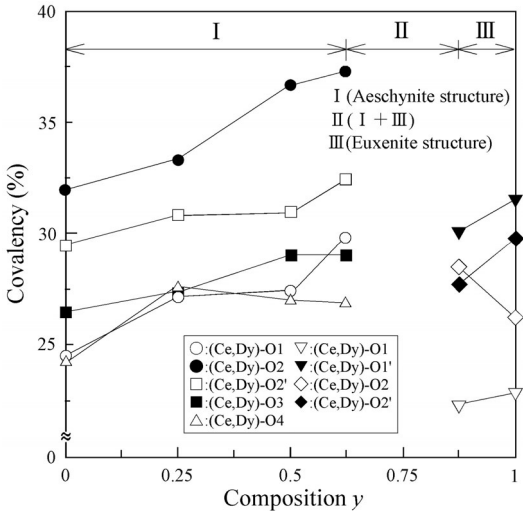
I
II
III
Ⅰ(Aeschynite structure)
Ⅱ(Ⅰ＋Ⅲ)
Ⅲ(Euxenite structure)
Covalency (%)
Composition y
○:(Ce,Dy)-O1
●:(Ce,Dy)-O2
□:(Ce,Dy)-O2'
■:(Ce,Dy)-O3
△:(Ce,Dy)-O4
▽:(Ce,Dy)-O1
▼:(Ce,Dy)-O1'
◇:(Ce,Dy)-O2
◆:(Ce,Dy)-O2'

Fig.8

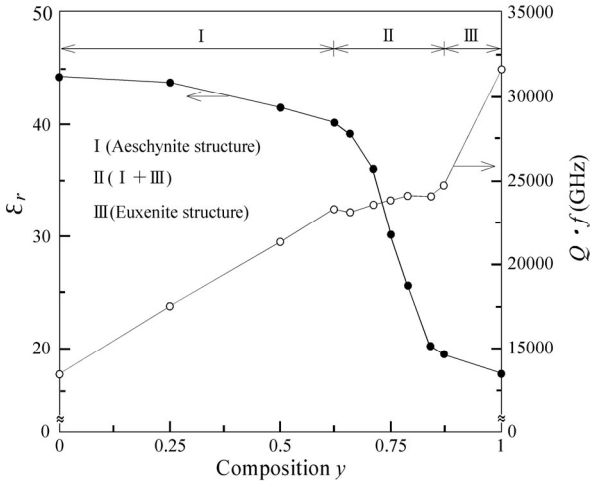
I
II
III
I (Aeschynite structure)
II (I + III)
III(Euxenite structure)
ε_r
$Q \cdot f$ (GHz)
Composition y
50
40
30
20
0
35000
30000
25000
20000
15000
0
0.25
0.5
0.75
1

Fig.9

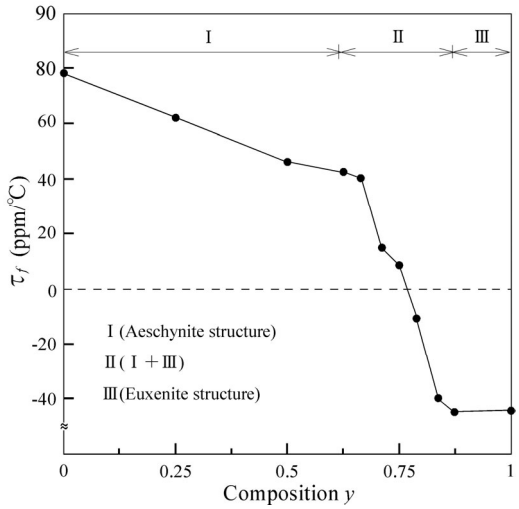
90
80
60
40
20
0
-20
-40
I
II
III
τ_f (ppm/°C)
I (Aeschynite structure)
II (I + III)
III (Euxenite structure)
0
0.25
0.5
0.75
1
Composition y

Fig.10

Table I
Microwave dielectric properties of $Ce(Nb_{1-x}Ta_x)TiO_6$ solid solutions.

Composition x	ε_r	$Q \cdot f$ (GHz)	τ_f (ppm/℃)
0	52.7	10702	91.8
0.1	50.4	11715	89.1
0.3	45.8	12498	85.6
0.5	44.6	13398	79.8
0.7	41.4	13885	74.8
0.9	38.3	14371	73.5
1	35.6	14616	72.0

Table II
Lattice parameters and unit cell volumes of $(Ce_{1-y}Dy_y)(Nb_{0.5}Ta_{0.5})TiO_6$ ceramics.

Crystal structure	Composition y	Lattice parameters (Å)			Unit cell volumes (Å^3)
		a	b	c	
Aeschynite	0	10.95809	7.54293	5.41107	447.258
	0.25	10.96686	7.50496	5.35890	441.069
	0.5	10.97443	7.46914	5.30998	435.257
	0.625	10.97520	7.44956	5.28293	431.934
Euxenite	0.875	14.65593	5.58497	5.21449	426.822
	1	14.63404	5.56684	5.20530	424.052